

MIXED ELECTROMECHANICAL SIMULATION OF ELECTROSTATIC MICROGENERATOR USING CUSTOM-SEMICONDUCTOR DEVICE MODELS

Kondala Rao. G, Paul D. Mitcheson, Tim C. Green

Department of Electrical Engineering, Imperial College London, UK.

Abstract: In this paper, modeling of semiconductors that are specially designed for power processing the output of an electrostatic microgenerator is presented and combined with an electromechanical system simulation of an electrostatic microgenerator. Various analytical expressions have been derived to study the effects of parasitic elements of semiconductor devices on electrostatic microgenerator effectiveness. These expressions are then used to estimate the likely operating regions (in terms of generator size and the acceleration of the source) over which the choice of the electrostatic transduction mechanism is sensible. It is shown that, whilst the electrostatic transducer itself is known to scale well to small sizes, when combined with the power processing circuit to form a microgenerator, this may not be the case.

Keywords: PSpice modeling, Electromechanical Simulations, Electrostatic Microgenerator, Effectiveness.

INTRODUCTION

To design a globally optimised electrostatic micro-generator, combined electromechanical PSpice simulations of electrostatic microgenerators have been previously carried out [1]. However in that work, ideal switch models were used for charging and discharging of the variable capacitor. It is important to use accurate semiconductor device models instead of ideal switches as it has been shown that the parasitics of the charge/discharge switches will significantly affect the capacitor voltage and therefore energy generation [2].

In this paper, PSpice modeling of the custom semiconductor devices (diode and MOSFET) designed in [2] is explained and an end-to-end system level simulations of the Coulomb Force Parametric Generator (CFPG) type electrostatic microgenerator is presented.

The effectiveness of an electrostatic microgenerator is plotted against generator size and input acceleration by assuming the microgenerator is cube shaped and the proof mass occupies half the volume. This is used in identifying the useful region of operation of a constant charge electrostatic microgenerator when interfaced with a power processing circuit.

MODELING OF CUSTOM SEMICONDUCTOR DEVICES

To achieve the high level of off-state impedance that is required to process the electrostatic microgenerator's output, semiconductor devices were specially designed with Silicon-On-Insulator (SOI) based technology [2]. Simulations of these devices were carried in Silvaco (finite element based software). However, these devices need to be modeled in PSpice in order

to allow a complete end-to-end system simulation to be run. Unfortunately, developing models in PSpice is not straight forward since these are power devices and PSpice inbuilt models do not accurately simulate some of the effects that are present in the power semiconductor devices (such as high level injection).

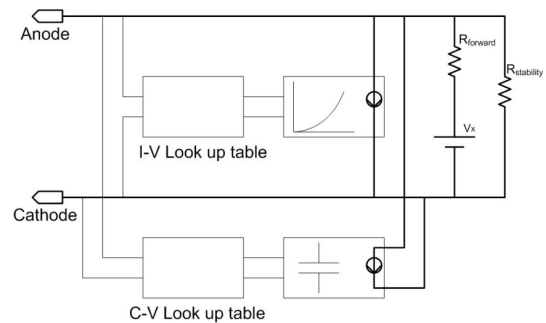


Fig. 1. Block diagram of Custom diode PSpice model

Whilst physics based models are useful for parameterising component models, they can be large and therefore slow to run in SPICE. Therefore, in this work, a look up table based method is used to model these custom devices in PSpice. Both diode and MOSFET are modeled using this method. Here, only the modeling of the diode is explained. Fig.1 shows the block diagram of the diode model with look-up tables. For instance, I-V characteristic data points of the custom diode are stored in the table. Then, by sensing the voltage between the anode and cathode, the corresponding current value from the table will flow in the current source. This simulates the diode forward characteristics. PSpice uses linear interpolation for

data points in the look-up table. However, PSpice will not extrapolate the characteristic values beyond the bounds of the stored data points. In order to maintain the continuity of the characteristics beyond those specified in the tables, extra components are added to the model. These are a voltage source V_x and a resistor $R_{forward}$ (valid because the series resistance is dominant after a certain forward voltage). The forward characteristics obtained using this model are shown in Fig.2. The PSpice simulation results closely match with the Silvaco data points.

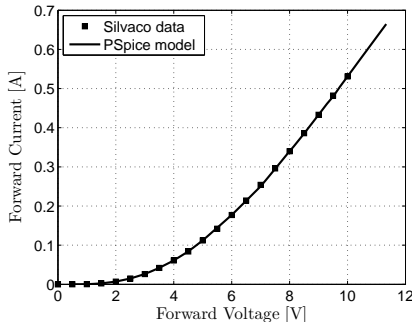


Fig. 2. Diode forward characteristics with look-up table based PSpice model

The diffusion and depletion capacitance characteristics of the custom diode are also stored in the look-up tables and are used to calculate the dynamic current source value by using $i = C(V) \times \frac{dV}{dt}$. This current source therefore represents the parasitic capacitance of the custom diode. Thereby, complete behavioral modeling of the custom diode has been achieved in an accurate and computationally efficient way.

ELECTROSTATIC MICROGENERATOR SYSTEM SIMULATIONS

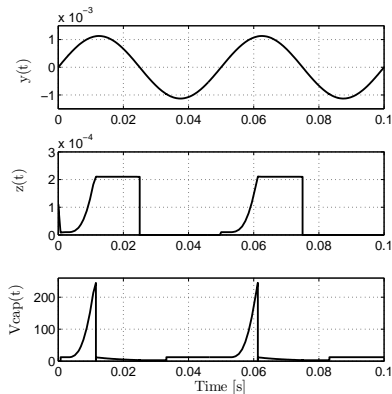


Fig. 3. Simulation results

Imperial College Energy-harvesting Simulator (ICES) toolkit [3] models are used to model mechanical parts of the CFPG microgenerator system and the transducer. The half-bridge converter that is proposed in [2] is used as power processing circuit. For simplicity, a load is not attached to the power converter output. Various simulation studies have been carried out and typical waveforms of input excitation ($y(t)$), proof mass displacement ($z(t)$) and the Variable capacitor voltage ($V_{cap}(t)$) are shown in Fig.3. It has been observed that the semiconductor device parasitic elements significantly effecting the variable capacitor voltage due to charge sharing and leakage.

Whilst these time domain simulations could be used to optimise the system, an analytical approach is required to speed up the process. This analysis will now be presented.

ANALYSIS OF ELECTROSTATIC MICROGENERATOR'S VOLTAGE WITH PARASITICS

In this section, a Coulomb Damped Resonant Generator (CDRG) type electrostatic microgenerator is considered for analysis and the variable capacitor voltage expressions (with and without parasitic elements) are derived. These expressions are then used in estimating the coupling effectiveness of the microgenerator and power conversion circuit efficiency. Finally, the effectiveness of the microgenerator is calculated under different operating conditions.

The optimal coulomb force of the CDRG with displacement constraint is given in [1] by:

$$F_{opt}cz = \frac{Y_0 \omega^2 m \omega_c}{|U|} \sqrt{\frac{1}{(1 - \omega_c^2)^2} - \frac{1}{\omega_c^4} \left(\frac{Z_l}{Y_0}\right)^2} \quad (1)$$

where $U = \frac{\sin(\frac{\pi}{\omega_c})}{1 + \cos(\frac{\pi}{\omega_c})}$, Y_0 is input excitation amplitude, m is mass of the generator proof-mass, Z_l is peak internal displacement, ω is angular frequency of the generator frame motion and $\omega_c = \frac{\omega}{\omega_n}$ and ω_n is generator natural frequency.

At resonance ($\omega_c = 1$), the optimal force is constant and Eq. 1 simplifies to:

$$F_{opt}cz = 0.7854mY_0\omega^2 \quad (2)$$

The electrostatic force between parallel plates of a capacitor for a given separation of $2Z_l$ is given by:

$$F_{electrostatic} = \frac{1}{2} \epsilon A_{plate} \left(\frac{V_{plate}}{2Z_l} \right)^2 \quad (3)$$

Where V_{plate} is capacitor voltage and A_{plate} is the area of the parallel plate.

The electrostatic microgenerator will be operating under optimal conditions, if the electrostatic force is equal to the coulomb force. Therefore, equating Eq. 2 and Eq. 3, we see that the maximum capacitor voltage is:

$$V_{plate} = 4.212 \times 10^5 (2Z_l) \sqrt{\frac{mY_o \omega^2}{A_{plate}}} \quad (4)$$

The above equation can be further simplified by assuming the microgenerator is cube shaped with side length of L_c and proof mass occupies half of the cube volume. Therefore, $m = \frac{\rho L_c^3}{2}$, $A_{plate} = L_c^2$, $2Z_l = \frac{L_c}{2}$, $\rho = 19300 \text{ Kg/m}^3$ (gold) and $Acc = Y_o \times \omega^2$. By substituting these values, the maximum capacitor plate voltage is simplified to:

$$V_{plate} = 2.07 \times 10^7 \sqrt{L_c^3 Acc} \quad (5)$$

Eq. 5 gives the microgenerator maximum voltage as a function of generator size and input acceleration. This is the ideal voltage since it is derived assuming there are no parasitic elements connected to the microgenerator capacitor.

When interfaced with a power processing circuit, the voltage generation of the microgenerator will be affected due to the parasitic elements such as off state leakage current and junction capacitance. In this paper, only parasitic capacitance is considered. Using analysis from [4] the junction capacitance can be expressed as:

$$C_j = \frac{A_{semi}}{2} \sqrt{\frac{2q\epsilon}{V_0 - V}} N_d \quad (6)$$

where C_j is junction capacitance, A_{semi} is area of the semiconductor, V_0 is built in potential and V is operating voltage, N_d is carrier doping density.

When the semiconductor devices are designed by choosing a doping density which minimises the on-state conduction losses per unit area ($N_d = \frac{14 \times 10^{22}}{V_B} m^{-3}$) [5], the junction capacitance is given by:

$$C_j = \frac{1.1 \times 10^{-3} A_{semi}}{\sqrt{(V_0 - V_{operation}) V_B}} \quad (7)$$

where $V_{operation}$, V_B are operating voltage and voltage blocking capacity of a semiconductor respectively.

Assuming the semiconductors are designed to block the maximum voltage of the microgenerator (given in Eq. 5), the semiconductor junction capacitance can be expressed as:

$$C_j = \frac{2.377 \times 10^{-7} A_{semi}}{\sqrt{(V_0 - V_{operation})} [L_c^3 Acc]^{\frac{1}{4}}} \quad (8)$$

The charge balance equation for a constant charge operation is given by:

$$C_{g1} \times V_{precharge} + C_{p1} \times V_{precharge} = C_{g2} \times V_{final} + C_{p2} \times V_{final} \quad (9)$$

where C_{g1} , C_{g2} are generator initial and final capacitances ($C_{g1} = \frac{\epsilon A_{plate}}{d_0}$, $C_{g2} = \frac{\epsilon A_{plate}}{2Z_l}$), C_{p1} and C_{p2} are initial and final parasitic capacitances, V_{final} is final voltage, $V_{precharge}$ is precharge voltage ($4.13 \times 10^7 d_0 \sqrt{L \times Acc}$) and d_0 is the initial separation of the plates.

After substituting these values in the Eq. 9 and simplifying; we obtain:

$$2\epsilon_0 L_c V_{final} + \frac{2.37 \times 10^{-7} A_{semi}}{[L_c^3 Acc]^{\frac{1}{4}}} \sqrt{V_{final}} = 3.6 \times 10^{-4} [L_c^3 Acc]^{\frac{1}{2}} + 1.5 \times 10^{-3} A_{semi} \sqrt{\frac{d_0}{L_c}} \quad (10)$$

Assuming $d_0 = 1 \mu m$, Eq. 10 has been solved analytically for V_{final} using Maple and is given by:

$$V_{final} = \frac{1}{[L_c^3 Acc]^{\frac{1}{2}}} \left[8.4 \times 10^{-6} [1.05 \times 10^{13} A_{semi}^2 - X_1 + X_2] \right] \quad (11)$$

Where

$$X_1 = 1.78 \times 10^{10} A_{semi} \sqrt{3.5 \times 10^5 A_{semi}^2 + 1.6 \times 10^5 [L_c^3 Acc] + 660 L_c^2 \sqrt{(Acc) A_{semi}}} \quad (12)$$

$$X_2 = 2.44 \times 10^{12} L_c^5 Acc + 10^{10} L_c^2 \sqrt{(Acc) A_{semi}} \quad (13)$$

Eq. 11 therefore gives an analytical expression for the microgenerator voltage when parasitic capacitance loading is present.

System effectiveness is defined as a product of coupling effectiveness and circuit efficiency.

The coupling effectiveness ($E_{coupling}$) is the ratio of the energy that is stored in the capacitor with and without parasitic elements present ($E_{coupling} = \frac{V_{final}^2}{V_{plate}^2}$) and the complete expression is given by:

$$E_{coupling} = \frac{1}{Acc^2 L_c^{10}} \left[1.6 \times 10^{-23} \left[1.69 \times 10^{13} A_{semi}^2 - X3 + X4 \right]^2 \right] \quad (14)$$

Where

$$X3 = 1.4 \times 10^9 A_{semi} \sqrt{1.4 \times 10^8 A_{semi}^2 + 4.05 \times 10^6 [L_c^5 Acc] + 66 \times 10^3 A_{semi} L_c^2 Acc^{0.5}} \quad (15)$$

$$X4 = 2.44 \times 10^{11} L_c^5 Acc + 4 \times 10^9 A_{semi} L_c^2 Acc^{0.5} \quad (16)$$

Circuit efficiency is a conventional efficiency. In any standard power processing circuit, the first stage of power conversion is transferring energy into an inductor and the efficiency of this stage is limited by the conduction losses of the switching element. Here, only this stage efficiency is estimated by assuming that the variable capacitor energy is transferred to the inductor through a resistance (MOSFET on state resistance, $R_{mosfet} = \frac{2 \times 10^{-11} V_B^2}{A_{semi}}$) and therefore this analysis provides an upper bound on circuit efficiency.

Coupling effectiveness, circuit efficiency and micro-generator effectiveness are plotted for different cube sizes and input accelerations (see Fig.4, Fig.5 and Fig.6 respectively). The optimal semiconductor area has been chosen for each and every point in order to maximise the system effectiveness.

As can be seen, the effectiveness increases with length. This is due to the fact that parasitic capacitance of pn junction is more at low voltages (inverse square root characteristics). At higher lengths and higher accelerations, the effectiveness falls slightly due to the increase in MOSFET drift region resistance at higher voltages.

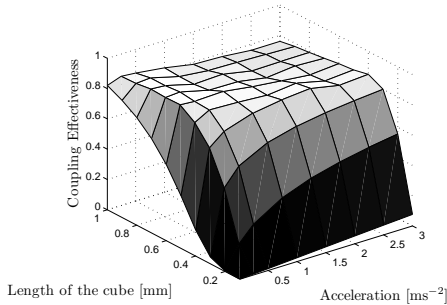


Fig. 4. Coupling effectiveness of an electrostatic microgenerator

CONCLUSIONS

End to end system simulations of CFPG type electrostatic microgenerator have been presented.

The effectiveness of an electrostatic microgenerator has been estimated and plotted against generator size

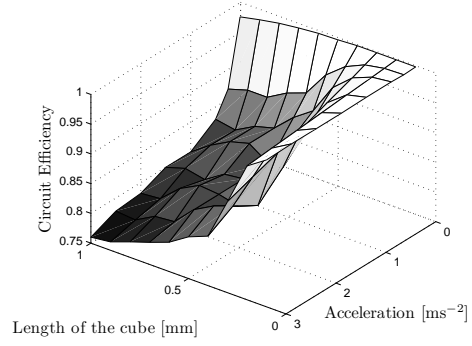


Fig. 5. Power Circuit Efficiency

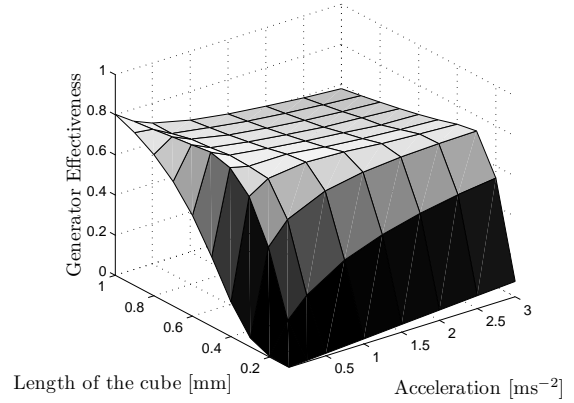


Fig. 6. Maximum effectiveness of an electrostatic microgenerator

and input acceleration. This plot is helpful in choosing the generator size for a given excitation.

In the analysis, factors such as off-state leakage current of semiconductor devices and complete power processing circuit are not considered. More accurate effectiveness can be estimated if these factors are considered. As can be seen, the effectiveness of an electrostatic microgenerator attached to a power processing circuit is relatively poor at small dimensions due to the relationship between capacitance and voltage in a pn junction.

REFERENCES

- [1] Mitcheson, P. D. Analysis and optimization of energy harvesting micro generator systems PhD thesis Department of Electrical Engineering, Imperial College London (2005).
- [2] Stark, B. H., Mitcheson, P. D., Miao, P., Green, T. C., Yeatman, E. M., and Holmes, A. S. (2006) *Power Electronics, IEEE Transactions on* **21(1)**, 27–37.
- [3] Kondala Rao, G., Mitcheson, P. D., and Green, T. C. November 2007 In Proceedings of PowerMEMS 2007 Freiberg, Germany: . pp. 137–140.
- [4] Streetman, B. G. and Banerjee, S. K. (2006) *Solid State Electronics Devices*, Pearson Prentice Hall, USA.
- [5] Duncan, A. G. and John, G. (1989) *POWER MOSFETS: Theory and Applications*, John Wiley & Sons, USA.